Polymer Chemistry

COMMUNICATION

View Article Online
View Journal | View Issue

Cite this: *Polym. Chem.*, 2017, **8**, 1999

Received 16th February 2017,
Accepted 2nd March 2017

DOI: 10.1039/c7py00270j

rsc.li/polymers

One-pot synthesis of reactive oxygen species (ROS)-self-immolative polyoxalate prodrug nanoparticles for hormone dependent cancer therapy with minimized side effects†

Anita Höcherl,*[a] Eliézer Jäger,*[a] Alessandro Jäger,[a] Martin Hrubý,[a] Rafał Konefał,[a] Olga Janoušková,[a] Jiří Spěváček,[a] Yaming Jiang,[b] Peter W. Schmidt,[b] Timothy P. Lodge[b] and Petr Štěpánek[a]

A new reactive oxygen species (ROS)-sensitive, self-immolative biodegradable polyoxalate prodrug based on the anticancer chemotherapeutic hormone analog diethylstilbestrol was synthesized *via* one-pot step-growth polymerization. The nanoparticles prepared from this prodrug undergo self-immolative degradation releasing the chemotherapeutic drug in ROS-rich environments, *e.g.*, in cancer cells. This new ROS self-immolative polyprodrug backbone eliminates the need for a linker between polymer chain and drug, resulting in a more specific drug release and minimized toxic side effects to non-ROS-producing cells as proven by *in vitro* experiments. The strategy enables re-utilization of a successful chemotherapeutic agent that has been clinically under-utilized due to dose-related side effects.

Introduction

Cancer is a leading cause of mortality worldwide, accounting for 8.2 million deaths in 2012, and it is expected that annual cancer cases will rise from 14 million in 2012 to 22 million within the next two decades.[1] In men, one of the five most common causes of death is due to cancers of the prostate.[1] Diethylstilbestrol (DEB, synthetic non-steroidal estrogen) has been a standard approach to the treatment of advanced prostate cancer for 50 years.[2] DEB is highly effective in prostate cancer treatment, with studies reporting that DEB has a similar efficacy to orchiectomy, at a daily dosage from 1 mg (low dose regime) to 3 mg.[2a–d] DEB was also successfully employed in estrogen additive therapy for women with estrogen receptor (ER)-positive metastatic breast cancer,[3] with studies showing that the survival of patients treated with daily 5 mg DEB was significantly higher than with Tamoxifen.[2d] However, DEB was eventually withdrawn from the clinical repertoire due to persistent severe dose-related toxicities, mainly cardiotoxicity.[2,3]

In recent years, the re-utilization of neglected and/or toxic drugs becomes possible by virtue of the encapsulation of drugs into lipid- or polymer-based nanoparticles (NPs) as *e.g.*, Doxorubicin encapsulated in liposomes (Doxil®) or through the synthesis of polymer–drug(protein) conjugates, *e.g.*, PEGaspargase (Oncaspar®).[4] Both approaches have proven clinically efficient in the treatment of several diseases. Despite this good efficiency, encapsulation can lead to drug leakage from the NPs during storage and blood circulation,[4] and most of the polymer–drug(protein) conjugates require the use of specific linkers and long synthetic pathways, *e.g.*, through acetal,[5] ester[6] or hydrazone[7] bonds. Consequently, polymer systems gain much more relevance in biomedical applications if they are tailored to be degradable in response to a stimulus, *e.g.*, light, pH change, or more recently, the elevated presence of ROS in cancer tissues.[8] The increased H_2O_2 production of cancer cells causes locally high peroxide concentrations, which can even exceed the oxidative burst of activated macrophages.[8d] This is due to imbalances in the ROS production (especially H_2O_2), and it leads to oxidative stress and activation of inflammation events, which can damage tissues and organs.[9]

Oxidation-responsive polymers and their relevant NPs including poly(propylene sulfide)s,[10] ferrocene-based,[11] boronic ester-based,[12] thioketal-based,[13] or polyoxalate-based[14] polymers have been prepared and studied for their potential in biomedical applications. Among these, the preparation of polymer systems sensitive to H_2O_2 through the cleavage of oxalate bonds is a particularly straightforward approach. Polymers containing oxalate bonds have been recently tested in murine models demonstrating interesting properties as antioxidants,[14a,b] as antioxidant-theranostic

[a]*Institute of Macromolecular Chemistry v.v.i., Academy of Sciences of the Czech Republic, Heyrovsky Sq. 2, 162 06 Prague 6, Czech Republic*
[b]*Department of Chemistry, University of Minnesota, 207 Pleasant Street SE, Minneapolis, MN, USA. E-mail: hocherl@imc.cas.cz, jager@imc.cas.cz*
†Electronic supplementary information (ESI) available. See DOI: 10.1039/c7py00270j

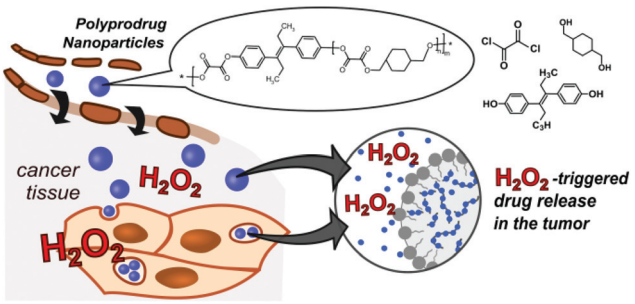

Scheme 1 Polyoxalate prodrug NPs (PDEB NPs) with self-immolative polymer degradation and DEB release in H_2O_2-rich tumor microenvironments.

agents,[14c] ischemia/reperfusion-targeted nanotherapeutics,[14d] and as nanoreactor systems for *in vivo* imaging of H_2O_2.[14c,d] Further attractive properties of the oxalate based polymers NPs include their degradation-induced luminescence (discussed hereafter) with tunable emission by the encapsulation of selected dyes, excellent specificity to H_2O_2 over other ROS species, deep-tissue imaging capabilities, and continuous detection of *in situ* produced H_2O_2 for long times.[14]

However no application for the treatment of cancer cells with this promising system has been reported yet. Herein, we describe a one-pot synthesis route to a novel self-immolative H_2O_2-sensitive polyprodrug material that provides biocompatibile and biodegradable nanoparticles with triggered degradation and chemotherapeutic drug release in ROS-rich environments (Scheme 1). The concept of polyprodrugs avoids the use of chemically specific linkers for drug release, by integrating the drug molecules into the polymer carrier backbone with stimuli-responsive bond and hyper-fast chain-breakage capabilities.[15]

Results and discussion

Polymers PDEB1, PDEB2, PDEB3

The three ROS self-immolative polyprodrug backbones with varied DEB amounts were synthesized by a one-pot step-growth polymerization. The reaction conditions were optimized and fine-tuned according to the molar ratio of the diols and the oxalyl chloride, in accordance with the reaction pathway detailed in the ESI† (see ESI† for methods). Briefly, diethylstilbestrol and 1,4-cyclohexanedimethanol (CHD) were dissolved in tetrahydrofuran (THF), and triethylamine was added dropwise at 4 °C. Afterwards oxalyl chloride dissolved in THF was added dropwise, and the polymerization reaction was continued for 6 hours at room temperature under nitrogen atmosphere. The resulting polyprodrugs were obtained by extraction using DCM and precipitation in cold hexane. Polyprodrugs with varied amounts of DEB (PDEB1 ~2.3 wt%; PDEB2 ~7.5 wt% and PDEB3 ~13.0 wt% of DEB) were obtained by varying the DEB, oxalyl chloride and CHD ratio (see Fig. S3 and ESI† for methods). The PDEBs were obtained as yellowish solids and the chemical structure was identified with ^{1}H NMR spectroscopy (Fig. 1A top and Fig. S1, ESI†). Successful polymer synthesis was confirmed by ^{1}H NMR (Fig. 1A top) and by size exclusion chromatography (SEC) analysis (Fig. S2, ESI†). The weight-average molecular weight (M_w) of polymer PDEB1 was 11.8 kDa with reasonable dispersity $M_w/M_n \approx 1.4$ as determined by SEC (Fig. S2, ESI†). No important differences in M_w were observed for PDEB2 and PDEB3 (Fig. S2, ESI†). The ^{1}H NMR spectrum of PDEB1 (Fig. 1A top, see ESI† for methods) shows the characteristic signals for protons belonging to the repeat units (see ESI† for peak assignments). Significantly lower mobility was revealed for aromatic protons of DEB units (signals a, b in Fig. 1A) in DMF-d_7 solutions of PDEB polyprodrugs in comparison with solution of the neat DEB from ^{1}H spin–spin relaxation times T_2 (see ESI† for measurements details), which in polyprodrugs (T_2 = 0.76 s) were twice shorter in comparison with the neat DEB (T_2 = 1.42 s). This fact together with the disappearance of the signal of DEB OH protons at 9.5 ppm in the spectra of the polyprodrugs (see ESI, Fig. S1B†) indicate that DEB units are covalently incorporated in the polymer chain. The degradation of PDEB1 as evaluated by ^{1}H NMR spectroscopy was complete after 3 days of incubation (Fig. 1A middle after 24 h and bottom after 72 h) as the broad peaks in ^{1}H NMR related to the polyprodrug are replaced by sharp peaks of the low-molecular-weight degradation products (monomers), confirming the self-immolative depolymerization triggered by H_2O_2.

Nanoparticles

With the aim to reduce the required dose, to minimize toxic side effects and to increase the specificity of DEB for cancer tissue, Tween-stabilized NPs based on the ROS self-immolative polyprodrug backbone PDEB1 were prepared (see ESI† for methods). Due to the incorporated oxalate linkers in the polyprodrug backbone, in an ROS-rich environment the polyprodrug will be self-immolatively degraded and the chemotherapeutic DEB released. We recently developed a NP drug-delivery system with H_2O_2-sensitive groups, which was able to deliver its drug cargo selectively to cancer cells (exploiting the higher level of peroxide in cancer cells compared to non-cancer cells).[12a] This approach is here refined with the insertion of the peroxide-sensitive oxalates as cleavable breakpoints integrated into the backbone as self-immolative polyprodrugs for selective drug release.

PDEB1 was chosen for *in vitro* evaluation (PDEB1 ~2.3 wt% of DEB, Fig. S3 and eqn (S3), ESI†) due to the superior stability of the PDEB1 NPs (see ESI† for methods). Dynamic light scattering (DLS) demonstrated NP stability in simulated physiological conditions and proved their peroxide-triggered degradation (Fig. 1B), and the degradation-triggered DEB release (Fig. S4, ESI†) specifically in simulated ROS-rich environments (H_2O_2). Note that the NPs were prepared to an average size of *ca.* 72 nm in diameter (hydrodynamic radius, $2R_H = D_H \approx$ 72 nm), *e.g.*, within a range known to be ideal for efficient tumor accumulation due to the EPR effect.[4,7]

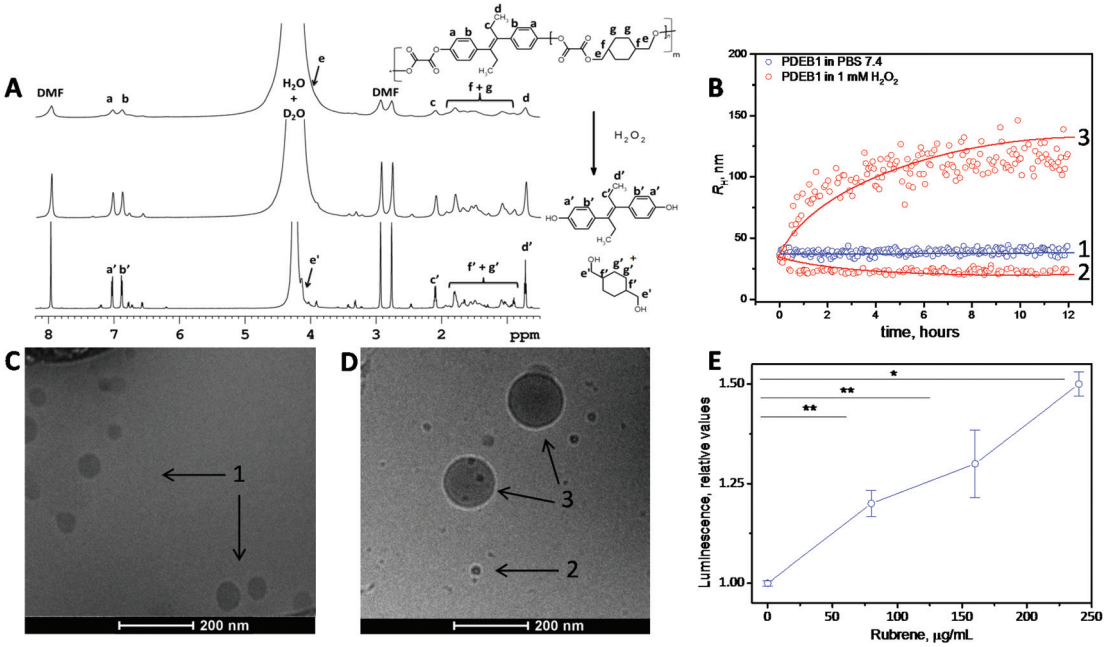

Fig. 1 (A) ^{1}H NMR spectra of the synthesized ROS self-immolative PDEB1 polyprodrug (before H_2O_2 addition in PBS/DMF-d_7) (top) and the degradation upon incubation with 1 mM of H_2O_2 after 24 h (middle) and 72 h (bottom). (B) Average R_H for PDEB1 polyprodrug NPs (blue – 1) with no H_2O_2 addition and after 12 h of incubation (red – 2 and 3) in 1 mM of H_2O_2 at 37 °C in PBS. (C) Cryo-TEM of the PDEB1 polyprodrug NPs before incubation with H_2O_2 and (D) after incubation with 1 mM H_2O_2 for 24 h. (E) Luminescence in MCF7 cancer cells after 2 h incubation with rubrene-loaded PDEB1 NPs, indicating the ROS-triggered cleavage of the oxalate groups in the polymer backbone. Sample '0 μg·mL^{-1} rubrene' corresponds to the NP-free control sample (*p < 0.01; **p < 0.03). The arrows in (C) and (D) correspond to the average R_H from the DLS in (B).

H_2O_2-Triggered polymer degradation

Under exposure to physiologically relevant levels of H_2O_2 [8a,12a] (250 μM, Fig. S4, ESI†) the oxalate groups of PDEB1 are oxidized and subsequently hydrolyzed triggering a self-immolative polymer backbone degradation releasing the chemotherapeutic DEB (see Scheme 1, Fig. 1B, S3 and S4, ESI†). The degradation of PDEB1 in the presence of H_2O_2 was also probed by cryo-TEM (Fig. 1C and D). Applying several different techniques, ^{1}H NMR spectra, DLS and the cryo-TEM images we showed that PDEB1 polyprodrug NPs degraded into small molecules and oligomers in a time- and H_2O_2-dependent manner. The larger objects observed in DLS and cryo-TEM during degradation (DLS in red Fig. 1B and cryo-TEM in Fig. 1D) most probably are related to the hydrophobicity of the polymer fragments that re-aggregate in solution due to the presence of the stabilizing agent and/or to NPs swollen due to the H_2O_2 attack.[16] Polymer degradation proceeds more extensively with increasing incubation time and H_2O_2 concentration (Fig. 1B and C and S5, ESI†). It is well established that the degradation of polyoxalate-based polymers induces chemiluminescence in peroxide-rich environments.[14,17] In this way the polymer degradation in cancer cells was demonstrated using PDEB1 polyprodrug NPs loaded with the dye rubrene (Fig. 1E), where the ROS-triggered cleavage of oxalate bounds induced rubrene luminescence (see Scheme S1, ESI† for proposed mechanism). The chemiluminescence was observed in MCF7 cancer cells (Fig. 1E) as well as in macrophages (see Fig. S6, ESI†), and the intensity of rubrene chemiluminescence correlated with the particle concentration, making the PDEB1 polyprodrug NPs useful for theranostics as well.[14c,17]

Cell viability testing

Taking into account previous works reporting the significantly higher cell viability for particles prepared from polyoxalates lacking DEB,[18] herein the cell viability experiments were performed with PDEB NPs. *In vitro* evaluation of the self-immolative PDEB1 polyprodrug NPs was performed in selected cell lines (see Fig. 2). Cell model systems for hormone therapy-treatable (LNCaP) and therapy-resistant (PC3) prostate cancer were used to evaluate the potential of PDEB1 in prostate cancer

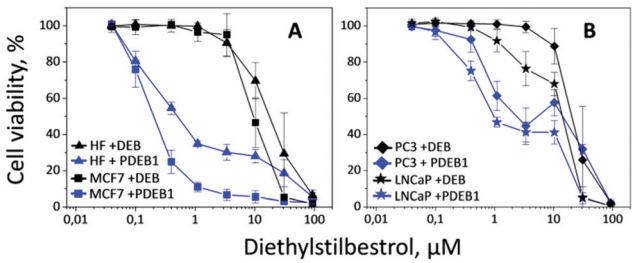

Fig. 2 Cell viability after 5 days incubation with the free drug DEB (black) and with the polyprodrug PDEB1 NPs (blue). The cell lines of HF (triangle) and MCF7 (square) are shown in (A), and of LNCaP (star) and PC3 (diamond) in (B).

treatment. Like all cancer cells, these cells have higher ROS levels, and PC3 and LNCaP produce up to 3-times more H_2O_2 than non-cancerous cells,[8d] thus being well suited to demonstrate the ROS-sensitive drug release of PDEB1. MCF7 cells were selected as a breast cancer model system, based on recent studies showing satisfactory results of DEB in the treatment of post-menopausal breast cancer.[2d,3] Human fibroblasts (HF) were used as a non-cancerous reference system. Cell viability after 5 days of incubation with PDEB1 polyprodrug NPs was evaluated using the AlamarBlue Assay (Fig. 2, see ESI† for methods and for DEB toxicity mechanism). The lower toxicity of the free, highly hydrophobic, drug compared to the drug-carrier system is a known effect and it is attributed both to the extensive adsorption of the hydrophobic drug molecules onto serum components such as serum albumin, whereas NPs drug carriers transport the drug directly into the cells[19a,b] and to the enhanced endocytotic uptake of polymer NPs when compared with the free drugs.[19c–h] HF cells produce a significantly lower level of ROS compared to the cancer cells,[8] hence the PDEB1 polyprodrug is degraded. However, as clearly visible in Fig. 2A, the ROS-sensitive polyprodrug NPs exerted a much higher toxicity on the cancer cells, MCF7, than on HF, while the free drug was equally toxic to cancer and non-cancer cells. Note that PDEB1 is specifically efficient *versus* the cancer cells in the low micromolar range, *i.e.*, at a concentration approximating the DEB blood plasma level in breast cancer therapy.[2d] Also for prostate cancer cells (Fig. 2B) LNCaP and even for the hormone-resistant PC3, PDEB1 polyprodrug NPs significantly lowered the required dose compared to the free drug. Similarly, the improved toxicity of PDEB1 was observed with cancer cell lines.[2c] PDEB1 also showed superior toxicity over the free drug.

Microscopy studies

Light microscopy revealed initial morphological changes and M-phase cell cycle arrest after 24 h incubation (and significant nuclear aneuploidy at >72 h) with PDEB1 polyprodrug NPs, while the free drug had no visible effect (data not shown). For the evaluation of morphological changes the cells were further studied after 24 h incubation with free DEB and PDEB1 NPs using confocal laser scanning microscopy (CLSM) (Fig. 3 and S7, ESI†). CLSM images in Fig. 3 show that the non-cancer cells (HF) were the least affected by PDEB1 polyprodrug NPs. HF displayed only an altered, less fibrous cell morphology and occasional nuclear fragmentation. Compared to that, cancer cell lines showed significant morphological changes such as nuclear fragmentation (indicating mitotic arrest) and aneuploidy (indicating G2/M arrest) in a high number of cells after incubation with PDEB1. The free drug did not have any visible toxic effects. Specifically LNCaP cells were strongly affected by PDEB1 in that most cells were detached, forming clusters (see Fig. S8†). This indicates a specific sensitivity of LNCaP to PDEB1 polyprodrug that results in disrupted cell adhesion, thereby promising additional cytotoxic effects in long-term, which adds to the attractiveness of PDEB1 polyprodrug for application in prostate cancer therapy. For further details on the microscopy studies, see ESI and Fig. S9.†

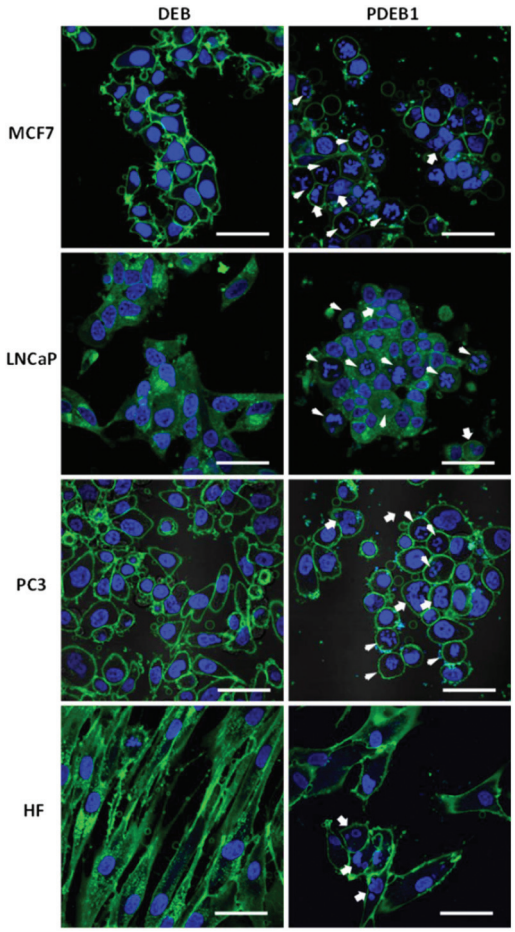

Fig. 3 Cells were incubated for 24 h with free DEB or PDEB1 NPs, at a total concentration of 3.4 μM DEB, to visualize nuclear fragmentation (arrow) and cells in mitotic arrest (arrowhead); nuclei were stained using Hoechst 33342 (blue) and the cytoplasmic membrane was labelled with CellMask™ (green). Scale bar = 50 μm.

Conclusions

The CLSM data correlates with the viability analysis, demonstrating again the enhanced toxicity of the PDEB1 prodrug against cancer cells. Note that the cytotoxicity of the PDEB1 polyprodrug NPs to HF cells was comparable to the toxicity of NPs prepared with the FDA-approved polymer polylactic acid PLA (Fig. S10, see ESI† for methods). The presented system shows great promise to achieve drug release specifically into tumors and lower the required drug dose in estrogen-dependent hormone therapy. In summary, for the first time a one-pot synthetic pathway to synthesize a new ROS self-immolative polyprodrug backbone based on the chemotherapeutic hormone analogue DEB is presented. The prepared NPs demonstrate higher activity against prostate and breast cancer cells *in vitro*, with lower activity in non-cancer cells due to the

selectivity to ROS-rich environments. Particle degradation in ROS-rich environments can be followed by chemiluminescence, opening the possibility for usage as theranostics. Finally the strategy presented here eliminates the need for a biodegradable linker. The NPs make it possible to reduce the side-effects of a highly effective and successful therapeutic molecule that was utilized for the treatment of hormone-dependent cancers, through a simple and efficient strategy.

Acknowledgements

The financial support of the Ministry of Education, Youth and Sports (grants # LH14079, POLYMAT #LO1507), the Czech Science Foundation (grant # 16-02870S, 15-13853S and 17-09998S), and the National Science Foundation through the University of Minnesota MRSEC, Award DMR-1420013 is gratefully appreciated.

Notes and references

1 World Health Organization (WHO), http://www.who.int/mediacentre/factsheets/fs297/en/ (July, 2016).
2 (*a*) S. B. Malkowicz, *Urology*, 2001, **58**, 108; (*b*) E. D. Crawford, *Rev. Urol.*, 2004, **6**, S3; (*c*) R. Turo, M. Smolski, R. Esler, M. L. Kujawa, S. J. Bromage, N. Oakley, A. Adeyoju, S. C. W. Brown, R. Brough, A. Sinclair and G. N. Collins, *Scand. J. Urol.*, 2014, **48**, 4; (*d*) P. P. Peethambaram, J. N. Ingle, V. J. Suman, L. C. Hartmann and C. L. Loprinzi, *Breast Cancer Res. Treat.*, 1999, **54**, 117; (*e*) H. A. Kemp, G. F. Read, D. Riad-Fahmy, A. W. Pike, S. J. Gaskell, K. Queen, M. E. Harper and K. Griffiths, *Cancer Res.*, 1981, **41**, 4693.
3 (*a*) R. Twombly, *J. Natl. Cancer Inst.*, 2011, **103**, 920; (*b*) J. N. Ingle, D. L. Ahmann, S. J. Green, J. H. Edmonson, H. F. Bisel, L. K. Kvols, W. C. Nichols, E. T. Creaan, R. G. Hahn, J. Rubin and S. Fryak, *N. Engl. J. Med.*, 1981, **304**, 16.
4 (*a*) T. Sun, Y. S. Zhang, B. Pang, D. C. Hyun, M. Yang and Y. Xia, *Angew. Chem., Int. Ed.*, 2014, **53**, 12320; (*b*) E. Jäger and F. C. Giacomelli, *Curr. Top. Med. Chem.*, 2015, **15**, 328.
5 J. Zou, G. Jafr, E. Themistou, Y. Yap, Z. A. P. Wintrob, P. Alexandridis, A. C. Ceacareanu and C. Cheng, *Chem. Commun.*, 2011, **47**, 4493.
6 A. G. Cheetham, Y.-C. Ou, P. Zhang and H. Cui, *Chem. Commun.*, 2014, **50**, 6039.
7 (*a*) K. Ulbrich, K. Holá, V. Šubr, A. Bakandritsos, J. Tuček and R. Zbořil, *Chem. Rev.*, 2016, **116**, 5338; (*b*) E. Jäger, A. Jäger, P. Chytil, T. Etrych, B. Říhová, F. C. Giacomelli, P. Štěpánek and K. Ulbrich, *J. Controlled Release*, 2013, **165**, 153.
8 (*a*) M. Giorgio, M. Trinei, E. Migliaccio and P. G. Pelicci, *Nat. Rev. Mol. Cell Biol.*, 2007, **8**, 722; (*b*) S. Toyokuni, K. Okamoto, J. Yodoi and H. Hiai, *FEBS Lett.*, 1995, **358**, 1; (*c*) T. P. Szatrowski and C. F. Nathan, *Cancer Res.*, 1991, **51**, 794; (*d*) B. Kumar, S. koul, L. Khandrika, R. B. Meacham and H. K. Koul, *Cancer Res.*, 2008, **68**, 177.
9 (*a*) A. Mantovani, P. Allavena, A. Sica and F. Balkwill, *Nature*, 2008, **454**, 436; (*b*) S. Reuter, S. C. Gupta, M. M. Chaturvedi and B. B. Aggarwal, *Free Radicals Biol. Med.*, 2010, **49**, 1603; (*c*) N. Houstis, E. D. Rosen and E. S. Lander, *Nature*, 2006, **440**, 944.
10 B. L. Allen, J. D. Johnson and J. P. Walker, *ACS Nano*, 2011, **5**, 5263.
11 (*a*) M. Hmyene, A. Yassar, M. Escorne, A. Percheron-Guegan and F. Garnier, *Adv. Mater.*, 1994, **6**, 564; (*b*) J. Tian, J. Chen, C. Ge, X. Liu, J. He, P. Ni and Y. Pan, *Bioconjugate Chem.*, 2016, **27**, 1518.
12 (*a*) E. Jäger, A. Höcherl, O. Janoušková, A. Jäger, M. Hrubý, R. Konefal, M. Netopilík, J. Pánek, M. Šlouf, K. Ulbrich and P. Štěpánek, *Nanoscale*, 2016, **8**, 6958; (*b*) C. de G. Lux, S. Joshi-Barr, T. Nguyen, E. Mahmoud, E. Schopf, N. Fomina and A. Almutairi, *J. Am. Chem. Soc.*, 2012, **134**, 15758.
13 (*a*) G. Saravanakumar, J. Kim and W. J. Kim, *Adv. Sci.*, 2016, 1600124; (*b*) D. S. Wilson, G. Dalmasso, L. Wang, S. V. Sitaraman, D. Merlin and N. Murthy, *Nat. Mater.*, 2010, **9**, 923.
14 (*a*) D. Jeong, C. Kang, E. Jung, D. Yoo, D. Wu and D. Lee, *J. Controlled Release*, 2016, **233**, 72; (*b*) S. Kim, H. Park, Y. Song, D. Hong, O. Kim, E. Jo, G. Khang and D. Lee, *Biomaterials*, 2011, **32**, 3021; (*c*) C. Kang, W. Cho, M. Park, J. Kim, S. Park, D. Shin, C. Song and D. Lee, *Biomaterials*, 2016, **85**, 195–203; (*d*) D. Lee, S. Park, S. Bae, D. Jeong, M. Park, C. Kang, W. Yoo, M. A. Samad, Q. Ke, G. Khang and P. M. Kang, *Sci. Rep.*, 2015, **5**, 16592.
15 (*a*) X. Hu, G. Liu, Y. Li, X. Wang and S. Liu, *J. Am. Chem. Soc.*, 2015, **137**, 362; (*b*) X. Hu, J. Hu, J. Tian, Z. Ge, K. Luo and S. Liu, *J. Am. Chem. Soc.*, 2013, **135**, 17617.
16 (*a*) A. Jäger, E. Jäger, F. Surman, A. Höcherl, B. Angelov, K. Ulbrich, M. Drechsler, V. M. Garamus, C. Rodriguez-Emmenegger, F. Nallet and P. Štěpánek, *Polym. Chem.*, 2015, **6**, 4946; (*b*) S. Petrova, E. Jäger, R. Konefał, A. Jäger, C. G. Venturini, J. Spěváček, E. Pavlova and P. Štěpánek, *Polym. Chem.*, 2014, **5**, 3884; (*c*) F. C. Giacomelli, P. Štěpánek, V. Schmidt, E. Jäger, A. Jäger and C. Giacomelli, *Nanoscale*, 2012, **4**, 4504.
17 (*a*) D. Lee, S. Khaja, J. C. Velasquez-Castano, M. Dasari, C. Sun, J. Petros, W. R. Taylor and N. Murthy, *Nat. Mater.*, 2007, **6**, 765; (*b*) D. Hong, B. Song, H. Kim, J. Know, G. Khang and D. Lee, *Ther. Delivery*, 2011, **2**, 1407.
18 (*a*) S. Cho, O. Hwang, I. Lee, G. Lee, D. Yoo, G. Khang, P. M. Kang and D. Lee, *Adv. Funct. Mater.*, 2012, **22**, 4038; (*b*) S. Kim, K. Seong, O. Kim, H. Seo, M. Lee, G. Khang and D. Lee, *Biomacromolecules*, 2010, **11**, 555; (*c*) H. Park, S. Kim, S. Kim, Y. Song, K. Seung, D. Hong, G. Khang and D. Lee, *Biomacromolecules*, 2010, **11**, 2103.
19 (*a*) D. A. Smith, L. Di and E. H. Kerns, *Nat. Rev. Drug Discovery*, 2010, **9**, 929; (*b*) A. I. Minchinton and I. F. Tannock, *Nat. Rev. Cancer*, 2006, **6**, 583; (*c*) G. Gaucher, R. H. Marchessault and J.-C. Leroux, *J. Controlled Release*,

2010, **143**, 2; (*d*) D. Li, Y. Zhang, S. Jin, J. Guo, H. Gao and C. Wang, *J. Mater. Chem. B*, 2014, **2**, 5187; (*e*) F. Danhier, N. Lecouturier, B. Vroman, C. Jérôme, J. Marchand-Brynaert, O. Feron and V. Préat, *J. Controlled Release*, 2009, **133**, 11; (*f*) H. S. Yoo, E. A. Lee and T. G. Park, *J. Controlled Release*, 2002, **82**, 17; (*g*) M. J. Vicent, R. Tomlinson, S. Brocchini and R. Duncan, *J. Drug Targeting*, 2004, **12**, 491; (*h*) V. Giménez, C. James, A. Armiñán, R. Schweins, A. Paul and M. J. Vicent, *J. Controlled Release*, 2012, **159**, 290.